Modulation of Src Kinase Activity by Selective Substrate Recognition with Pseudopeptidic Cages

Lucía Tapia,[a] Naiara Solozabal,[b] Jordi Solà,[a] Yolanda Pérez,[b] W. Todd Miller,*[c] and Ignacio Alfonso*[a]

Abstract: The selective recognition of tyrosine residues in peptides is an appealing approach to inhibiting their tyrosine kinase (TK)-mediated phosphorylation. Herein, we describe pseudopeptidic cages that efficiently protect substrates from the action of the Src TK enzyme, precluding the corresponding Tyr phosphorylation. Fluorescence emission titrations show that the most efficient cage inhibitors strongly bind the peptide substrates with a very good correlation between the binding constant and the inhibitory potency. Structural insights and additional control experiments further support the proposed mechanism of selective supramolecular protection of the substrates. Moreover, the approach also works in a completely different kinase-substrate system. These results illustrate the potential of supramolecular complexes for the efficient and selective modulation of TK signaling.

Introduction

The tyrosine kinase (TK) signaling cascade represents a complex phosphorylation reaction network that is fundamental for understanding cell function.[1] The dysregulation of certain TKs is related to serious diseases like neurological disorders,[2] diabetes[3] and cancer.[4] Thus, the central role of TKs in cell regulation and disease has encouraged the design of synthetic molecules able to modulate TK activity.[5] One successful approach has been ATP competitive TK inhibitors, which have shown clinical efficacy in several cases. For example, treatment of human chronic myelogenous leukemia with imatinib, an ATP competitive inhibitor, results in remission in nearly 100% of newly diagnosed patients in the early stages.[6] However, designing specific kinase inhibitors is challenging due to the high conservation of the ATP binding pocket.[7] Even clinically successful inhibitors can act on multiple kinases; for example, imatinib was found to bind 26 kinases.[8] This promiscuity limits the effectiveness of many potential inhibitors.[9] Moreover, very often, a given TK phosphorylates different protein substrates within the whole network, meaning that the putative inhibition of its enzymatic activity will impact several signaling and regulation pathways.[10] A complementary way to modulate TK activity is the selective binding of the Tyr residue in the protein or peptide substrate, protecting it from the action of the enzyme (Figure 1A).

The realization of this mechanism requires the strong and selective recognition of a peptide side chain under physiologically relevant conditions (i.e., aqueous buffer at neutral pH),

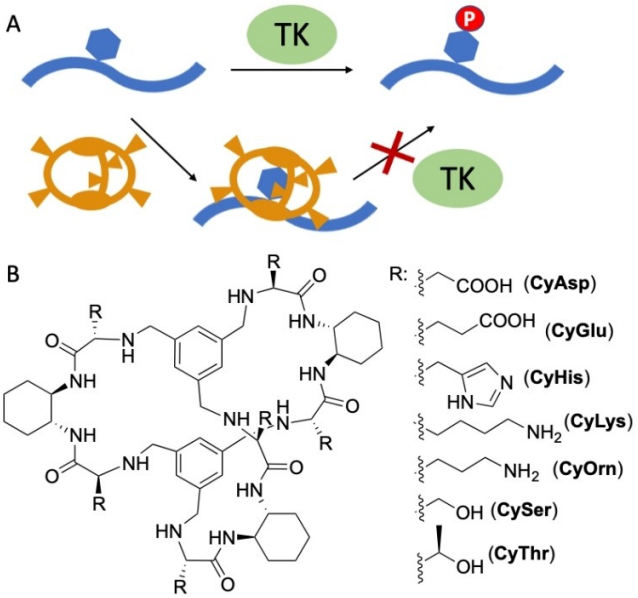

Figure 1. A) Schematic representation of the proposed mechanism for substrate-recognition TK modulation. B) Chemical structures of the pseudopeptidic cages used in this work.

[a] L. Tapia, Dr. J. Solà, Dr. I. Alfonso
Department of Biological Chemistry
Institute for Advanced Chemistry of Catalonia, IQAC-CSIC
Jordi Girona 18–26, 08034, Barcelona (Spain)
E-mail: ignacio.alfonso@iqac.csic.es

[b] N. Solozabal, Dr. Y. Pérez
NMR Facility
Institute for Advanced Chemistry of Catalonia, IQAC-CSIC
Jordi Girona 18–26, 08034, Barcelona (Spain)

[c] Prof. Dr. W. T. Miller
Department of Physiology and Biophysics, Stony Brook University and
Department of Veterans Affairs Medical Center
Stony Brook, NY, 11794 and Northport, NY 11768 (USA)
E-mail: todd.miller@stonybrook.edu

Supporting information for this article is available on the WWW under https://doi.org/10.1002/chem.202100990

which is an extremely challenging task in supramolecular chemistry.[11] Consequently, the approach in Figure 1A has been scarcely tested. In a previous contribution[12] we reported on the use of certain pseudopeptidic macrobicycles (CyLys and CyOrn in Figure 1B) able to inhibit the TK-promoted phosphorylation, as shown by a TK commercial kit that employs the unnatural universal polyE$_4$Y substrate. Later on, cationic pillarenes were also used in a very similar fashion.[13] Although these preliminary results demonstrated the proof of concept, the important issue of substrate selectivity still remains unaddressed. Only very recently, Zhao and co-workers reported the use of molecularly imprinted nanoparticles able to inhibit serine kinases by substrate binding, though the method was less effective in Tyr protection.[14]

Based on our previous results, we envisioned that the selective TK-modulation properties of our cages could be harnessed by the additional recognition of the residues surrounding the Tyr in the peptide substrates. To test that idea, we designed cages bearing different chemical functional groups facing the exterior (acidic, basic and nonionizable polar functions), while keeping the inner cavity of the hosts as the binding pocket for the Tyr (Figure 1B). As the benchmark TK, we chose Src for its wide substrate acceptance and biological relevance in cell physiology and cancer.[15]

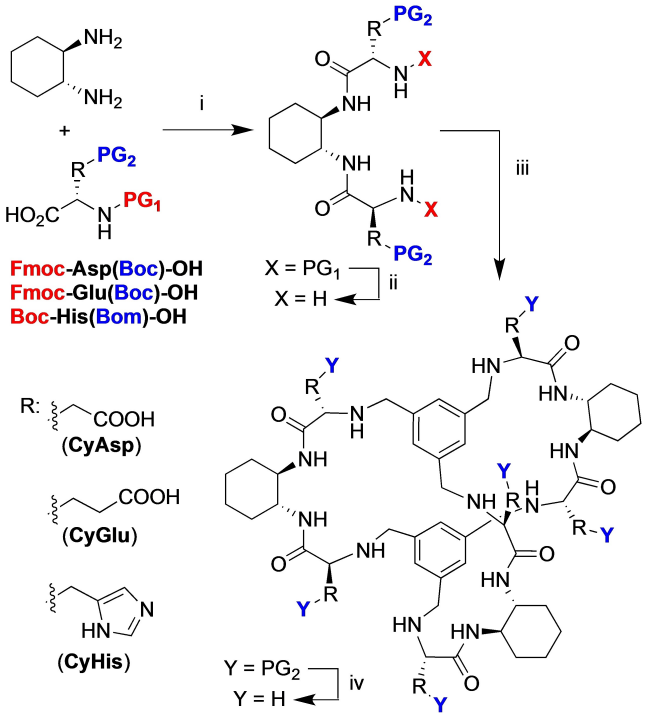

Scheme 1. General pathway for the synthesis of the pseudopeptides cages: i) HBTU, DIPEA in DMF; ii) piperidine in DMF (Asp and Glu) or TFA/TES in CH_2Cl_2 (His); iii) benzene-1,3,5-tricarbaldehyde in MeOH (12 h at RT) and then $NaBH_4$; iv) TFA/TES in CH_2Cl_2 (Asp) or H_3PO_4/TES in CH_2Cl_2 (Glu) or TFA/TFMSA/*p*-cresol (His).

Results and Discussion

The corresponding cages were synthesized according to the general procedure depicted in Scheme 1. The key macrobicyclization is a [3+2] reductive amination reaction, where the structural preorganization of the bis(amidoamine) precursor governs the process.[16] The rest of the steps in the synthetic scheme correspond to amide coupling and orthogonal deprotection reactions as in conventional solution phase peptide synthesis. Thus, the preparation of CySer/CyThr,[17] and CyLys/CyOrn[12] was previously described by us, while CyAsp, CyGlu and CyHis are new receptors, for which synthetic and characterization details are given in the Supporting Information.

In order to study the effect of these cages on Src kinase activity, we used the phosphocellulose paper binding assay.[18] Initially we tested polyE$_4$Y as the reference nonspecific substrate, which showed that all the cages inhibit the kinase activity of Src to some degree (Figure 2A). However, we observed significant differences between the receptors, with the Asp, Lys and Orn cages being the most active ones. The activity observed with CyLys and CyOrn is in agreement with our previous results using a TK commercial kit,[12] and can be explained by the electrostatic attraction between their cationic side chains and the negatively charged polypeptide sequence that mediate substrate recognition. The performance of CyAsp was counterintuitive following the same rationale, and must be due to other factors (see below).

For a deeper study of the substrate selectivity, we tested a series of synthetic peptides: the Src peptide substrate identified by Cantley and co-workers (Src-PS),[19] a sequence derived from the Wiskott-Aldrich syndrome protein (WASP)[20] and the Ile5Val mutant of the hormone Angiotensin II (V5Ang-II)[21] (Figure 2B). They differ in several structural aspects, such as their length, hydrophobicity and charge distribution along the sequence. A Gly6Ala variant of Src-PS (A6Src-PS) was also considered to check the effect of a single substitution close to the phosphorylation site with minimal structural perturbation. The protection of the Tyr residues from the Src-promoted phosphorylation depends on both the cage structure and the peptide sequence (Figure 2C–F). As a general trend, CyAsp is the most efficient phosphorylation inhibitor, leading to almost complete inhibition in the case of Src-PS and A6Src-PS (Figure 2C and D, blue bar) and to >50% inhibition with the other peptide substrates (Figure 2E and F). The cages made from Lys, Orn and His also show interesting activities with marked differences between substrates.

The comparison between CyLys and CyOrn is especially noteworthy, as the relative inhibitory activities vary for the different peptides (compare yellow and purple bars in Figure 2C and F). Thus, CyLys inhibits Src-PS phosphorylation more efficiently than CyOrn, while for Va5Ang-II the trend is significantly reversed (WASP lies in between). Even more remarkably, CyHis displays a noticeable activity only for the V5Ang-II substrate (Figure 2F, green bar), being comparable with the best inhibitors in this case, CyAsp and CyOrn (blue and purple bars, respectively). Overall, the observed differences suggest that the inhibitory activity occurs by the selective encapsulation of the Tyr side chain of the peptide substrates,

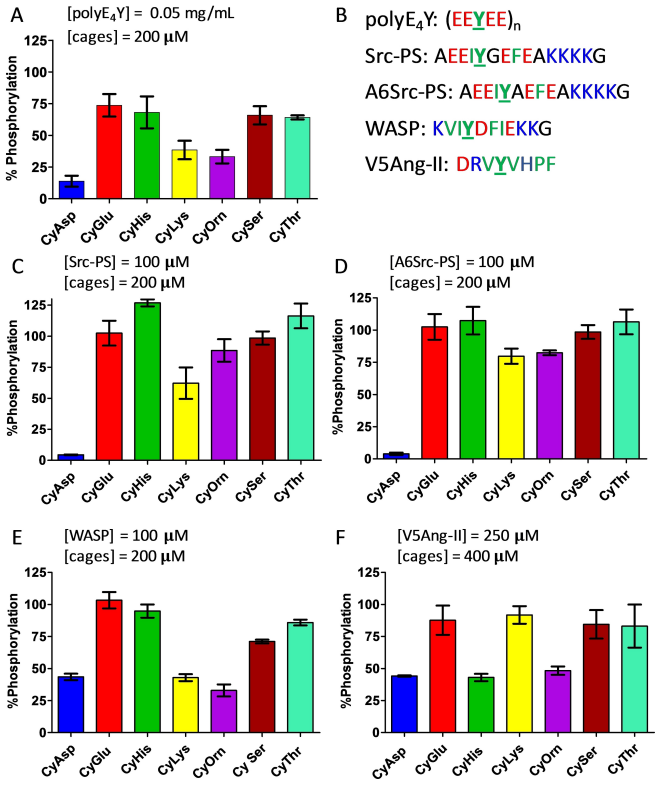

Figure 2. A) Effect of the cages on the Src-promoted Tyr phosphorylation of the polyE$_4$Y substrate. B) Peptide sequences used in this work. Effect of the cages on the Src-promoted Tyr-phosphorylation of the substrates C) Src-PS, D) A6Src-PS, E) WASP and F) V5Ang-II. In all cases, the plots show the percentage phosphorylation relative to the corresponding control reactions in the absence of a cage.

which depends on the accessory interactions between the side chains of the different cages and the amino acid side chains surrounding the Tyr residue.

As the cage-substrate interaction is a key factor in the inhibitory activity, we decided to study the supramolecular structures for selected cages by exploiting the changes in fluorescence emission of the Tyr side chain upon inclusion inside the cage cavity[12] (Table 1).

The first important observation is the nonlinear concentration dependence of the fluorescence emission of the peptides in solution. Fitting the dilution titration data rendered a relatively strong dimerization constant for the three studied peptides (Table 1, entry 1), which implies their effective self-assembly at μM concentrations, such as those used in the phosphorylation assays. These dimerization processes were taken into account in all the equilibria shown below.

Regarding the cage-peptide binding, the fluorescence titrations show important differences between the systems. Thus, the fitting of the fluorescence titration data with CyAsp (entry 2) requires considering the formation of [CyAsp-Mg-peptide] ternary complexes (Figure 3). The CyAsp-Mg interaction was independently confirmed by ^{1}H NMR titration experiments (K_{Mg}, entry 3 in Table 1, Figures S56 and S57). Besides, the corresponding fluorescence titration experiments in the absence of Mg salt only showed dynamic quenching and a weaker binding (Figure S48), confirming the key role of the Mg^{II} ion in the peptide-cage interaction. For a fair comparison, the corresponding equilibrium constants for the binding of the [CyAsp-Mg] species to the peptides (K_1^{Mg}) are included in entry 4 of Table 1. In all the cases this interaction is very strong ($K_1^{Mg} \approx 2–4\times10^4\ M^{-1}$), explaining the efficient inhibition by CyAsp of the Src-catalyzed phosphorylation reactions, which were performed in a relatively high concentration of Mg ions.

Rather surprisingly, the binding mode with CyGlu was found to be simpler (entry 5). In this case, the Mg ion does not directly intervene in the formation of the supramolecular complexes, which was additionally confirmed by control titration experiments at low Mg concentration (compare Figures S49 and S50). The different Mg^{II} coordination trends of Asp/Glu amino acids explains the behavior observed for CyAsp and CyGlu.[22] Thus, Mg^{II} could form a 6-membered ring chelate with the amino and carboxylate groups in the case of CyAsp, which is not possible with CyGlu.

Remarkably, CyGlu rendered much lower cage-peptide binding constants (at least one order of magnitude, compare entries 4 and 5 in Table 1), which is in very good agreement with its poorer phosphorylation inhibition abilities.

The case of CyHis is more difficult to rationalize, because all the tested peptides lead to complexes with 1:1 and 1:2

Table 1. Logarithm of the equilibrium constants (logβ, log$K$) for the complexes formed by A) peptides, B) cages and C) the Mg^{II} ion obtained by fluorescence titration upon excitation at 276 nm (30 mM Tris buffer at pH 7.5 and 20 mM $MgCl_2$). Values in parentheses correspond to the standard deviation of the last significant figure, and the corresponding reaction equation defining each equilibrium is included in each case.

Entry	Cage	Reaction	Property	Src-PS	WASP	V5Ang-II
1	peptide[a]	$2A \leftrightarrows A_2$	$\log\beta(\text{dimer}) = \log K_{dim}$[a]	4.97(3)	5.20(3)	3.56(2)
2	CyAsp	$A+B+C \leftrightarrows ABC$	$\log\beta(ABC)$	5.24(3)	5.640(3)	5.30(1)
3	CyAsp	$B+C \leftrightarrows BC$	$\log K_{Mg}$[b]	0.95(3)[b]	0.95(3)[b]	0.95(3)[b]
4	CyAsp	$A+BC \leftrightarrows ABC$	$\log K_1^{Mg}$	4.29	4.69	4.35
5	CyGlu	$A+B \leftrightarrows AB$	$\log\beta(AB) = \log K_1$	3.258(6)	3.306(3)	2.844(6)
6	CyHis	$A+2B \leftrightarrows AB_2$	$\log\beta(AB_2)$	6.45(1)	6.61(2)	6.53(1)
7	CyHis	$A+B \leftrightarrows AB$	$\log\beta(AB) = \log K_1$	3.697(6)	3.89(2)	3.44(1)
8	CyHis	$AB+B \leftrightarrows AB_2$	$\log K_2$	2.75	2.72	3.09
9	CyHis	not applicable	$\alpha = 4\ K_2/K_1$[c]	0.45	0.27	1.79
10	CyLys	$A+B \leftrightarrows AB$	$\log\beta(AB) = \log K_1$	3.82(3)	3.447(6)	2.80(1)
11	CyOrn	$A+B \leftrightarrows AB$	$\log\beta(AB) = \log K_1$	3.489(4)	3.537(6)	3.419(3)

[a] Corresponding to the dimerization of the peptide. [b] Obtained by ^{1}H NMR titration experiments. [c] Cooperativity parameter as defined in ref. [24].

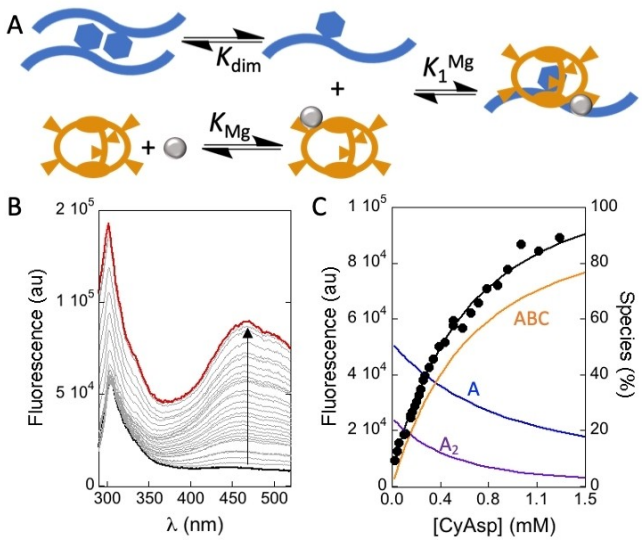

Figure 3. A) Binding mode of peptides to the CyAsp-Mg species. The peptide is shown in blue, the cage is orange, and the Mg^{II} ion is depicted as a silver sphere. B) Fluorescence emission spectra of Src-PS peptide (black, 10 μM, 30 mM Tris buffer at pH 7.5, 20 mM $MgCl_2$) upon increasing concentrations of CyAsp (gray to red). C) Fluorescence at 467 nm (experimental values as black symbols, fitting line) and species concentrations: free Src-PS (blue), dimer (purple) and [CyAsp-Mg-Src-PS] complex (orange).

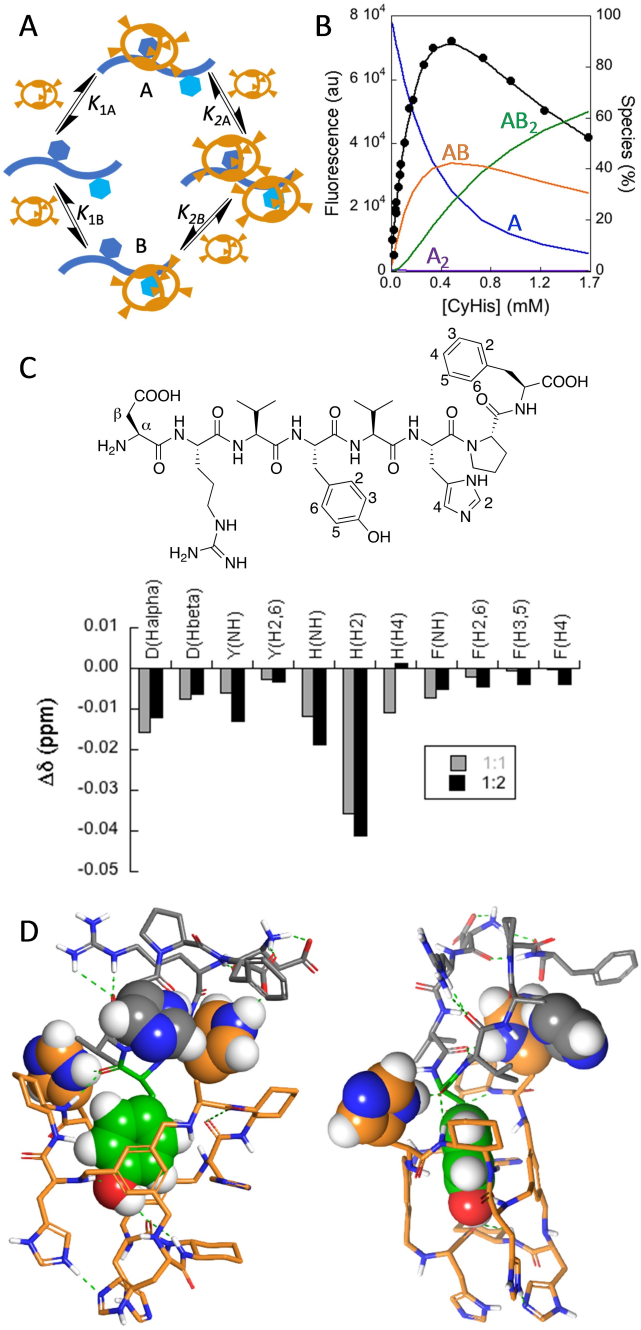

Figure 4. A) Schematic representation of the binding mode for the CyHis receptor (orange), implying 1:1 and 1:2 supramolecular complexes. The peptide is shown in blue. Dimerization of the peptide is omitted for simplicity. B) Fluorescence (442 nm) titration of V5Ang-II (black, 1 μM, 30 mM Tris buffer at pH 7.5, 20 mM $MgCl_2$) upon addition of CyHis: observed fluorescence (•), fitting (line); equilibrium species: free V5Ang-II (blue), dimer (purple), 1:1 (orange) and 1:2 (green) complexes. C) Plot of the chemical-shift perturbation of the ^{1}H NMR signals of V5Ang-II upon binding to CyHis under the conditions for the main formation of the 1:1 (gray) and 1:2 (black) peptide/cage complexes. D) Two views of the proposed [CyHis-V5Ang-II] supramolecular complex (Macro Model OPLS3e minimized structure). The cage C atoms are shown in orange, and the Tyr4 V5Ang-II C-atoms are shown in green, most nonpolar H atoms are omitted for clarity, and selected aromatic rings are displayed as CPK. H-bonds are represented as green dashed lines.

peptide/CyHis stoichiometry (entry 6). Cages of this type can recognize other aromatic residues, although the Phe binding is usually weaker.[23] Our titration data show that CyHis is less selective for Tyr than the other receptors, binding to both aromatic residues (Tyr and Phe) present in the three peptidic substrates. This equilibrium scheme requires a more careful analysis: Table 1 shows the corresponding stepwise constants for the individual binding events (entries 7 and 8). Moreover, for the 1:1 supramolecular species, there are two possible micro-species (A and B in Figure 4A) leading to encapsulation of either Tyr or Phe residues. This is very relevant, since the Phe-bound species would be less efficient in the Tyr protection. In such complex processes, the evaluation of the cooperativity parameter[24] is highly convenient (α in entry 9). Thus, the recognition of Src-PS and WASP by CyHis shows the usual negative cooperativity ($\alpha < 1$) meaning that the first binding event hinders the second one. This can be reasonably explained by electrostatic and steric repulsions between consecutive binding of two CyHis to close residues in the peptide sequence. Thus the peptide with closer Tyr/Phe residues (WASP) also shows lower α value, reflecting this hindering effect. However, for V5Ang-II-CyHis, an uncommon positive cooperativity ($\alpha > 1$) implies that the first CyHis binding favors the formation of the 1:2 complex. This remarkable difference could account for the different inhibitory abilities in the phosphorylation assays. In most cases (i.e., Src-PS and WASP), CyHis binding to Phe sequesters the cage and reduces Tyr protection, whereas CyHis inhibits the phosphorylation of the V5Ang-II substrate either through a Tyr encapsulation in the 1:1 complex or by a cooperative Tyr encapsulation following the initial Phe binding.

In order to better understand this singular behavior, we prepared samples that maximize the 1:1 and 1:2 V5Ang-II/CyHis supramolecular complexes to compare their ^{1}H NMR spectra with that of the peptide alone. The chemical shift perturbations of the peptide ^{1}H NMR signals (Figure 4C) show upfield shifts of the Asp1, Tyr4 and His6 signals in the 1:1 complex (gray bars in Figure 4C), while the aromatic protons of Phe8 are shielded mainly in the 1:2 complex (black bars in Figure 4C). These results strongly suggest the Tyr4 residue as the site for the first binding event.

A structural proposal for this complex is shown in Figure 4D (also see Figures S66 and S67). In agreement with the changes observed in the fluorescence emission spectra, the Tyr4 aromatic side chain (green CPK in Figure 4D) fits inside the cage cavity, favoring the interaction of the surrounding amino acids with the receptor. In this minimum, the *i*Pr groups of Val3 and Val5 lay on top of two cyclohexane rings of CyHis, possibly establishing hydrophobic contacts. On the other hand, since Tyr4 and His6 are correlated in Ang-II-type peptides,[25] the presence of Tyr4 within the host cavity causes His6 to approach to one of the imidazole rings of CyHis (highlighted CPK in Figure 4D) in an edge-to-face disposition that explains the shielding observed in the His6 ^{1}H NMR signals, especially for H2 (Figure 4C). The complex is additionally stabilized by six host-guest H-bonds, mainly implicating Tyr4 from the guest and the imidazole rings from the host. For instance, two cage His residues bind the backbone amide carbonyls of Val3 and Tyr4 from V5Ang-II. This model illustrates how the Tyr4 inclusion within the cage cavity is enforced by additional interactions between side chains, thus explaining why CyHis is particularly efficient in the inhibition of V5Ang-II phosphorylation.

The binding data obtained with CyLys and CyOrn are especially significant (entries 10 and 11 in Table 1). Thus, CyLys binds to Src-PS more strongly than CyOrn, with the corresponding inhibition showing the same trend (CyLys > CyOrn, Figure 2C). However, the binding of WASP peptide to CyOrn is slightly stronger than to CyLys, with the same order in the inhibition experiments (CyOrn > CyLys, Figure 2E). Finally, the recognition of V5Ang-II peptide is fivefold more efficient with CyOrn than with CyLys, which is clearly reflected in the phosphorylation experiments, where CyOrn is a more potent inhibitor (Figure 2F). Thus, for these two structurally similar cages, CyLys and CyOrn, the binding and the inhibitory efficiencies are strongly correlated. The higher basicity of CyLys renders a more positively charged host than CyOrn at neutral pH, on average.[12] On the other hand, the number of negatively charged residues in the studied substrates varies in the series: Src-PS > WASP > V5Ang-II. Thus, the attractive secondary electrostatic interactions favor the complexes with CyLys also in the same trend, giving a reasonable explanation to both the binding and inhibition results.

Overall, although the direct comparison between substrates must be done carefully due to the intrinsic dimerization properties of the sequences and distinct Src affinities, our cage-peptide binding data successfully explain the observed trends in the phosphorylation assays.

With the aim of confirming the proposed inhibition mechanism, we performed additional phosphorylation experiments. First, we considered the potential competition of a protein displaying several solvent-exposed Tyr residues. We examined the effect of bovine serum albumin (BSA), which is commonly included in phosphorylation assays to prevent nonspecific hydrophobic interactions. BSA contains 20 Tyr residues, of which at least 12 are located at the protein surface or in an accessible pocket (PDB ID: 4F5S). The presence of BSA reduces the inhibitory ability of the cages (Figures S31 and S32), suggesting a competitive effect of the Tyr residues of BSA through partial complexation of the cages. The corresponding BSA-cage interaction was also confirmed by additional NMR experiments (Figure S65). Nevertheless, the observation of inhibition activities even in the presence of competing BSA implies a stronger binding of the cages to the target peptides. We also built a dose-response curve for the CyAsp/Src-PS pair, at three different concentrations of the peptide substrate (Figure 5). Remarkably, the calculated IC_{50} of CyAsp is proportional to the concentration of Src-PS at a constant concentration of Src, which means that the cage inhibits the phosphorylation through the specific supramolecular peptide recognition. These additional results further support the inhibition mechanism depicted in Figure 1A.

In order to validate the generality of the approach, we tested our strategy in a completely different TK-system: the insulin-like growth factor 1 receptor (IGF1R) and the KKEEEE**Y**MMMMG peptide substrate (E4YM4).[26] Several of the cages inhibited the Tyr phosphorylation, with CyAsp and CyHis being the most potent ones in this case (Figure 6A). These activities can be also explained with the corresponding supramolecular complexes. Thus, also in this case, a very stable [CyAsp-Mg-E4YM4] species was confirmed by fluorescence titration (Figure 6B) rendering a $\log\beta(ABC) = 5.406(3)$ and $\log K_1^{Mg} = 4.46$. On the other hand, the fluorescence titration of E4YM4 with CyHis can be successfully fitted to a simpler 1:1 binding mode ($\log\beta(AB) = 3.784(8)$), in agreement with the absence of a second aromatic amino acid in the substrate. This

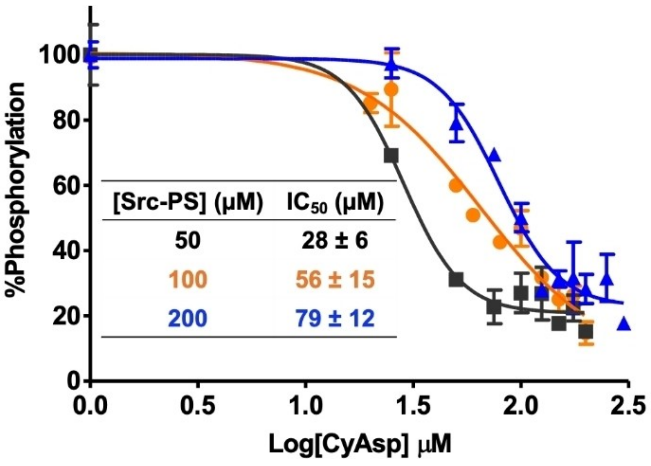

Figure 5. Dose-response plot for the CyAsp inhibition of the Src-mediated phosphorylation of different concentrations of Src-PS substrate.

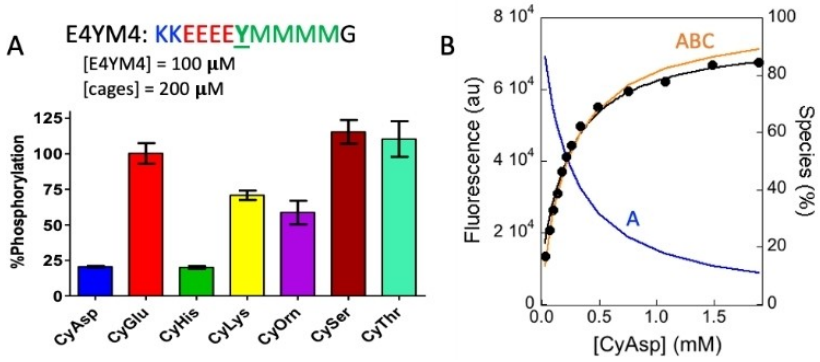

Figure 6. A) Effect of the cages on the IGF1R-promoted Tyr phosphorylation of E4YM4 (the plots show the percentage phosphorylation relative to the corresponding control reactions in the absence of a cage). B) Fluorescence emission (465 nm) of E4YM4 (black, 10 μM, 30 mM Tris buffer at pH 7.5, 20 mM $MgCl_2$) upon increasing the concentration of CyAsp.

strong binding also explains the ability of CyHis to inhibit the IGF1R-promoted phosphorylation of E4YM4.

Conclusion

Our results demonstrate that the supramolecular binding of tyrosine residues in peptides represents an efficient method to protect the substrates from TK-mediated phosphorylation. The inhibitory activities can be rationalized by considering the cage-peptide complexes; this supports the proposed mechanism. The binding constants and the inhibitory activities are modulated by the secondary interactions established between the side chains of the peptide substrates and the cages, which complement the binding of Tyr within the cage cavity. This approach paves the way to the selective modulation of an individual kinase-stimulated signaling pathway without interfering with other functions of the kinase, thus potentially leading to the development of improved tools for research, diagnosis, or therapy in biomedicine.

Experimental Section

Materials: Reagents and solvents were purchased from commercial suppliers (Adrich, Fluka or Merck) and were used without further purification. Compounds CySer, CyThr, CyLys and CyOrn were synthetized as previously described.[12,17] Details for the synthesis of CyAsp, CyGlu and CyHis are provided in the Supporting Information. A general procedure for the key macrocyclization reaction is exemplified for the synthesis of CyAsp. The open-chain bis (amidoamine) precursor (0.3 g, 0.657 mmol) was dissolved in anhydrous MeOH (25 mL). Benzene-1,3,5-tricarbaldehyde (0.071 g, 0.42 mmol) was added. The solution was stirred at room temperature for 24 h. Then $NaBH_4$ (0.116 g, 4.38 mmol) was added and the reaction mixture was stirred for 24 h more. After reaction was completed, NH_4Cl (aq) was added to neutral pH and the product was extracted with CH_2Cl_2. The resulting crude was purified by column chromatography (CH_2Cl_2/MeOH 95:5). The white solid obtained was dissolved in CH_2Cl_2/TFA 1:1 (2 mL) with 0.2 mL of triethylsilane (TES). The solution was stirred for 3 h. After, TFA was evaporated and the solid was washed several times with diethyl ether. Final product was purified by reverse phase chromatography. CyAsp was obtained as a TFA salt (white solid, 35% yield). All the compounds prepared were fully characterized by the complete spectroscopic (NMR, ESI-MS) and analytical data. Preparative reverse phase purifications were performed on an Isolera Biotage instrument (KP-C18-HS, CH_3CN and water with 0.1% TFA). Analytical RP-HPLC was performed with a Hewlett Packard Series 1100 (UV detector 1315A) modular system using a reverse-phase Kromasil 100 C_8 (15×0.46 cm, 5 μm) column. CH_3CN-H_2O mixtures containing 0.1% TFA at 1 mL/min were used as mobile phase and monitoring wavelengths were set at 220, 254 and 280 nm.

NMR spectroscopy: The NMR experiments were carried out at 25 °C on a V NMRS-400 NMR spectrometer (Agilent Technologies 400 MHz for ^1H and 100 MHz for ^{13}C) for characterization and a Bruker Avance-III 500 MHz spectrometer equipped with a *z*-axis pulsed field gradient triple resonance (^1H, ^{13}C, ^{15}N) TCI cryoprobe (500 MHz for ^1H and 125 MHz for ^{13}C) for further interaction studies. Chemical shifts are reported in ppm using tetrakis(trimethylsilyl) silane as a reference. Data were processed with the software program MNova11 (Mestrelab Research).

ESI mass spectrometry: High resolution mass spectra (HRMS) were performed on Acquity UPLC System and a LCT PremierTM XE Benchtop orthogonal acceleration time-of-flight (oa-TOF; Waters Corporation) equipped with an electrospray ionization source. All sample solutions (over the 1×10^{-4} to 1×10^{-6} M range) were prepared in methanol.

Kinase activity assays: Src Kinase catalytic domain was expressed and purified from *Escherichia coli* as described[27] and was a kind gift from Dr. Markus Seeliger (Stony Brook University). The IGF1R kinase domain was purified from *Spodoptera frugiperda* Sf9 cells using a recombinant baculovirus as described.[28] Radioactivity measurements were conducted in a HIDEX-300 SL scintillation counter. For assaying PTK (protein tyrosine kinase) activities, we measured the phosphorylation of the different polypeptides using the acid precipitation onto filter paper assay.[18,29] Phosphorylation reactions were conducted in Eppendorf tubes with a total volume of 25 μL per reaction. Each reaction mixture contains Tris buffer (30 mM, pH 7.5), 20 mM $MgCl_2$, 400 μM ATP, peptide (Src-PS, WASP or Val5-AngII at the desired concentration), the cage (at different concentrations depending on the assay), ^{32}P-ATP (0.1 μL, 10 mci/mL) and SRC (at the optimal concentration for each substrate). Each reaction mixture was incubated at 30 °C for 5–10 min. At the end of the reaction time, 5 μL of trichloroacetic acid were added to the reaction Eppendorf and the solution was centrifuged. Then 35 μL of

the supernatant were spotted onto a 2×2 cm Whatman filter paper which was subsequently washed in 5% H_3PO_4 3 times for 10 min each time followed by a final wash with acetone. Finally, each paper's radioactivity was determined by scintillation counting. The assay conditions (peptide concentrations, enzyme concentrations and incubation time) for each peptide were accurately optimized to ensure that the selected ones fall within the linear phase of the enzymatic reaction. Conditions: PolyE_4Y: 10 min incubation, 50 nM Src and 0.1 mg/mL of the polypeptide; Src-PS and A6Src-PS: 7 min incubation, 10 nM Src and 100 μM of the polypeptide; WASP: 10 min incubation, 50 nM Src and 100 μM polypeptide; V5Ang-II: 15 min incubation, 200 nM Src and 250 μM polypeptide. Results were expressed as % of phosphorylation compared to the control experiments (assay without the cage compound) so controls were considered to be the 100%. Each plot is a representation of the average of at least 3 repetitions and error bars correspond to the standard deviation. Kinase inhibition assays with the system E_4YM_4: The kinase inhibition activity of the cage compounds was tested with a different kinase/peptide system as a control experiment for the action mechanism proposed. The system selected was the peptide E_4YM_4: (whose sequence is KKEEEE**Y**MMMMG) with the IGF1R kinase. The assay was conducted with 0.64 μM IGF1R and 100 μM polypeptide, and the incubation time was set to 10 min (Figure 6A).

Fluorescence spectroscopy: Fluorescence emission spectra were acquired on a SpectraMax M5 instrument using 10 mm path length cuvettes, excitation bandwidth: 9 nm, emission bandwidth: 15 nm, light source: Xenon flash lamp (1 J/flash), emission read every 1 nm. All the fluorescence experiments were performed at 20 °C and specific measuring details and fitting procedures are given in the corresponding section for each titration example. The different peptide-cage titrations were all conducted in a 700 μL fluorescence cuvette following the following protocol: A solution of the peptide (100, 10 or 1 μM) was prepared in buffered water (30 mM Tris, pH 7.5, 20 mM $MgCl_2$). 300 μL of the peptide solution was titrated with a solution of the cage (1-3 mM) in buffered water (30 mM Tris, pH 7.5, 20 mM $MgCl_2$) containing the titrated peptide in the same concentration (100, 10 or 1 μM) to maintain the peptide concentration constant throughout the whole titration. The peptide concentration was adjusted for each titration to the concentration that prevents precipitation events and allows to get a larger number of meaningful experimental points for the fitting. The excitation wavelength was λ_{ex}: 276 nm and the emission window recorded was adjusted for each peptide to acquire the whole emission bad for the excimer λ_{em} 290–500/550 nm.

Fitting procedure: HypSpec[30] software was used to fit the fluorescence titration data to every proposed interaction model. This software performs the global fitting of the whole emission band (or a selected range) for each titration point, to satisfy the interaction model in each case. This model can include several association constants between 1, 2 or more components. In these particular cases the peptides emission fluorescence spectra were first measured in a wide concentration range and, for those showing a nonlinear emission versus concentration plot, a simple dimerization model was used to extract K_{dim}. Next, the titration of a fixed concentration of the peptides with increasing amount of the cages was carried out. For the peptides prone to dimerize, K_{dim} was included in the fitting process of the cage-peptide titration as a constant value, and the corresponding cage-peptide stability constant $\beta(AB_n)$ was obtained from the fitting. As a default, the simplest 1:1 binding mode was tested and, if necessary, a more complex 1:2 binding mode was used (CyHis). In the specific case of CyAsp, the formation of a Mg^{II} complex was considered. For that, the CyAsp-Mg^{II} interaction was measured by ^{1}H NMR titration and the corresponding K_{Mg} was obtained by fitting the data using HypNMR.[31] Accordingly, the obtained K_{Mg} was included as a constant value in the fitting of the fluorescence emission titrations of all the peptides with CyAsp. Although this method performs a global fitting of the whole emission band, Figures 3C, 4B and 6B only show the fitting of a single wavelength for simplicity.

Acknowledgements

Financial support from the Spanish Ministry of Science and Innovation (RTI2018-096182-B-I00, RED2018-102331-T, MCI/AEI/FEDER, EU), AGAUR (2017 SGR 208) and personal support for L.T. (BES-2016-076863) are gratefully acknowledged. This work was also supported by US Department of Veterans Affairs Merit Award BX002292 to W.T.M. We acknowledge support of the publication fee by the CSIC Open Access Publication Support Initiative through its Unit of Information Resources for Research (URICI).

Conflict of Interest

The authors declare no conflict of interest.

Keywords: cages · peptides · phosphorylation · supramolecular chemistry · tyrosine kinases

[1] M. D. Haskell, J. K. Slack, J. T. Parsons, S. J. Parsons, *Chem. Rev.* **2001**, *101*, 2425–2440.
[2] a) J. Ma, T. Jiang, L. Tan, J.-T. Yu, *Mol. Neurobiol.* **2014**, *51*, 820–826; b) R. Abbassi, T. G. Johns, M. Kassiou, L. Munoz, *Pharmacol. Ther.* **2015**, *151*, 87–98; c) A. F. T. Arnsten, *Nat. Neurosci.* **2015**, *18*, 1376–1385.
[3] a) C. Louvet, G. L. Szot, J. Lang, M. R. Lee, N. Martinier, G. Bollag, S. Zhu, A. Weiss, J. A. Bluestone, *Proc. Nat. Acad. Sci. USA* **2008**, *105*, 18895–18900; b) A. Fountas, L.-N. Diamantopoulos, A. Tsatsoulis, *Trends Endocrinol. Metab.* **2015**, *26*, 643–656.
[4] a) J. B. Casaletto, A. I. McClatchey, *Nat. Rev. Cancer* **2012**, *12*, 387–400; b) C. Pottier, M. Fresnais, M. Gilon, G. Jérusalem, R. Longuespée, N. E. Sounni, *Cancers* **2020**, *12*, 731.
[5] a) A. J. Bridges, *Chem. Rev.* **2001**, *101*, 2541–2572; b) N. Berndt, R. M. Karim, E. Schönbrunn, *Curr. Opin. Chem. Biol.* **2017**, *39*, 126–132; c) R. Roskoski, Jr., *Pharmacol. Res.* **2016**, *103*, 26–48.
[6] B. J. Druker, *Cancer Cell* **2002**, *1*, 31–36.
[7] S. M. Hanson, G. Georghiou, M. K. Thakur, W. T. Miller, J. S. Rest, J. D. Chodera, M. A. Seeliger, *Cell Chem. Biol.* **2019**, *26*, 390–399.
[8] M. W. Karaman, S. Herrgard, D. K. Treiber, P. Gallant, C. E. Atteridge, B. T. Campbell, K. W. Chan, P. Ciceri, M. I. Davis, P. T. Edeen, R. Faraoni, M. Floyd, J. P. Hunt, D. J. Lockhart, Z. V. Milanov, M. J. Morrison, G. Pallares, H. K. Patel, S. Pritchard, L. M. Wodicka, P. P. Zarrinkar, *Nat. Biotechnol.* **2008**, *26*, 127–132.
[9] Q. Jiao, L. Bi, Y. Ren, S. Song, Q. Wang, Y.-S. Wang, *Mol. Cancer* **2018**, *17*, 36.
[10] a) W. T. Miller, *Acc. Chem. Res.* **2003**, *36*, 393–400; b) C. J. Miller, B. E. Turk, *Trends Biochem. Sci.* **2018**, *43*, 380–394.
[11] a) W. C. Still, *Acc. Chem. Res.* **1996**, *29*, 155–163; b) M. W. Peczuhand, A. D. Hamilton, *Chem. Rev.* **2000**, *100*, 2479–2494; c) R. E. McGovern, H. Fernandes, A. R. Khan, N. P. Power, P. B. Crowley, *Nat. Chem.* **2012**, *4*, 527–533; d) L. C. Smith, D. G. Leach, B. E. Blaylock, O. A. Ali, A. R. Urbach, *J. Am. Chem. Soc.* **2015**, *137*, 3663–3669; e) J. E. Beaver, M. L. Waters, *ACS Chem. Biol.* **2016**, *11*, 643–653; f) S. van Dun, C. Ottmann, L.-G. Milroy, L. Brunsveld, *J. Am. Chem. Soc.* **2017**, *139*, 13960–13968; g) Z. Hirani, H. F. Taylor, E. F. Babcock, A. T. Bockus, C. D. Varnado, Jr., C. W. Bielawski, A. R. Urbach, *J. Am. Chem. Soc.* **2018**, *140*, 12263–12269; h) B. D. Smith, *Synthetic Receptors for Biomolecules: Design Principles and Applications*, The Royal Society of Chemistry, **2015**.

[12] E. Faggi, Y. Perez, S. V. Luis, I. Alfonso, *Chem. Commun.* **2016**, *52*, 8142–8145.
[13] C.-P. Li, Y.-X. Lu, C.-T. Zi, Y.-T. Zhao, H. Zhao, Y.-P. Zhang, *Int. J. Mol. Sci.* **2020**, *21*, 4979.
[14] X. Li, T. M. Palhano Zanela, E. S. Underbakke, Y. Zhao, *J. Am. Chem. Soc.* **2021**, *143*, 639–643.
[15] a) G. S. Martin, *Nat. Rev. Mol. Cell Biol.* **2001**, *2*, 467–475; b) H. Krishnan, W. T. Miller, G. S. Goldberg, *Genes Cancer* **2012**, *3*, 426–435; c) R. Roskoski, Jr. *Pharmacol. Res.* **2015**, *94*, 9–25; d) V. Jha, M. Macchia, T. Tuccinardi, G. Poli, *Cancers* **2020**, *12*, 2327; e) S. Martellucci, L. Clementi, S. Sabetta, V. Mattei, L. Botta, A. Angelucci, *Cancers* **2020**, *12*, 1448; f) A. Simatou, G. Simatos, M. Goulielmaki, D. A. Spandidos, S. Baliou, V. Zoumpourlis, *Mol. Clin. Oncol.* **2020**, *23*, 21.
[16] A. Moure, S. V. Luis, I. Alfonso, *Chem. Eur. J.* **2012**, *18*, 5496–5500.
[17] E. Faggi, C. Vicent, S. V. Luis, I. Alfonso, *Org. Biomol. Chem.* **2015**, *13*, 11721–11731.
[18] J. E. Casnellie, *Methods Enzymol.* **1991**, *200*, 115–120.
[19] a) Z. Songyang, K. L. Carraway III, M. J. Eck, S. C. Harrison, R. A. Feldman, M. Mohammadi, J. Schlessinger, S. R. Hubbard, D. P. Smith, C. Eng, M. J. Lorenzo, B. A. J. Ponder, B. J. Mayer, L. C. Cantley, *Nature* **1995**, *373*, 536–539; b) N. Yokoyama, W. T. Miller, *FEBS Lett.* **1999**, *456*, 403–408.
[20] a) N. Yokoyama, J. Lougheed, W. T. Miller, *J. Biol. Chem.* **2005**, *280*, 42219–42226; b) N. Yokoyama, W. T. Miller, *Methods Enzymol.* **2006**, *406*, 250–260.
[21] T. W. Wong, A. R. Goldberg, *J. Biol. Chem.* **1983**, *258*, 1022–1025.
[22] H. Schmidbaur, H. G. Classen, J. Helbig, *Angew. Chem. Int. Ed. Engl.* **1990**, *29*, 1090–1103; *Angew. Chem.* **1990**, *102*, 1122–1136.
[23] E. Faggi, A. Moure, M. Bolte, C. Vicent, S. V. Luis, I. Alfonso, *J. Org. Chem.* **2014**, *79*, 4590–4601.
[24] P. Thordarson, *Chem. Soc. Rev.* **2011**, *40*, 1305–1323.
[25] N. Zhou, G. J. Moore, H. J. Vogel, *J. Protein Chem.* **1991**, *10*, 333–343.
[26] S. Favelyukis, J. H. Till, S. R. Hubbard, W. T. Miller, *Nat. Struct. Biol.* **2001**, *8*, 1058–1063.
[27] P. Pellicena, D. S. King, A. M. Falick, J. Kuriyan, M. A. Seeliger, M. Young, M. N. Henderson, *Protein Sci.* **2005**, *14*, 3135–3139.
[28] M. Z. Cabail, S. Li, E. Lemmon, M. E. Bowen, S. R. Hubbard, W. T. Miller, *Nat. Commun.* **2015**, *6*, 6406.
[29] C. J. Hastie, H. J. McLauchlan, P. Cohen, *Nat. Protoc.* **2006**, *1*, 968–971.
[30] P. Gans, A. Sabatini, A. Vacca, *Talanta* **1996**, *43*, 1739–1753; http://www.hyperquad.co.uk/HypSpec2014.htm.
[31] a) C. Frassineti, S. Ghelli, P. Gans, A. Sabatini, M. S. Moruzzi, A. Vacca, *Anal. Biochem.* **1995**, *231*, 374–382; b) C. Frassineti, L. Alderighi, P. Gans, A. Sabatini, A. Vacca, S. Ghelli, *Anal. Bioanal. Chem.* **2003**, *376*, 1041–1052; http://www.hyperquad.co.uk/hypnmr.htm.

Manuscript received: March 18, 2021
Accepted manuscript online: April 27, 2021
Version of record online: June 1, 2021

